

# Modelling the dynamic response and failure modes of reinforced concrete structures subjected to blast and impact loading

Tuan Ngo<sup>†</sup> and Priyan Mendis

*Infrastructure Protection Research Group, Department of Civil & Environmental Engineering,  
University of Melbourne, VIC 3010, Australia*

*(Received February 22, 2009, Accepted April 14, 2009)*

**Abstract.** Responding to the threat of terrorist attacks around the world, numerous studies have been conducted to search for new methods of vulnerability assessment and protective technologies for critical infrastructure under extreme bomb blasts or high velocity impacts. In this paper, a two-dimensional behavioral rate dependent lattice model (RDLM) capable of analyzing reinforced concrete members subjected to blast and impact loading is presented. The model inherently takes into account several major influencing factors: the progressive cracking of concrete in tension, the inelastic response in compression, the yielding of reinforcing steel, and strain rate sensitivity of both concrete and steel. A computer code using the explicit algorithm was developed based on the proposed lattice model. The explicit code along with the proposed numerical model was validated using experimental test results from the Woomera blast trial.

**Keywords:** concrete; blast loading; impact; lattice model; finite element method; high strain-rate.

---

## 1. Introduction

The numerical simulation of the real behavior in the nonlinear finite element method lies primarily in the improvements of the constitutive models of materials. At present, a considerable number of models are available for the nonlinear behavior of reinforced concrete under compressive stress, for the long-term behavior of concrete, for simulating crack initiation and propagation, etc. However less attention has been paid to the modeling of strain rate sensitivity of concrete and steel reinforcement under impulsive loading. The analytical prediction of failure modes of reinforced concrete structures under severe impulsive loads is very difficult, due to the complexity of concrete behavior in the high strain-rate domain. As a result of the impulsive loads reaching their peak intensity in extremely short durations of time, material nonlinearities and strain-rate effects play an important role in the analysis. Most current design and analysis methods are based on simplified equivalent static forces or single degree of freedom systems. Although this approach may be suitable for preliminary analysis, it contains inherent inconsistencies. The finite element method

---

<sup>†</sup> Ph.D., Corresponding author, E-mail: [dtngo@unimelb.edu.au](mailto:dtngo@unimelb.edu.au)

provides an effective numerical approach for the modelling of structural problems involving severe impulsive loading. Thus, one of the main aims of this study is to improve the realism of these models, and to account for the strain rate sensitivity to predict the nonlinear structural response of two-dimensional concrete structures subject to impulsive loading.

The Rate Dependent Lattice Model (RDLM) for concrete and steel, developed in this study, is based on a strain rate sensitive concrete and reinforcement material model in tension and compression and is suitable for the two-dimensional analysis of RC structures. Major sources of nonlinearities in reinforced concrete structures has been taken into consideration, such as the progressive cracking of concrete in tension, the inelastic response in compression, the yielding of reinforcing steel, and strain-rate sensitivity of concrete and steel reinforcement. The smeared crack approach is employed to model concrete cracking behavior. Steel reinforcement is modelled as a strain rate dependent elasto-viscoplastic material. Material nonlinearities including crack propagation, concrete crushing, post-failure residual strength, as well as the strain rate effects on the response of concrete and steel can be modelled by the proposed explicit code developed in this study.

The explicit code is validated using experimental test results from the Woomera blast trial and other test data available from literature. Numerical analysis and a parametric study of reinforced concrete structures subjected to impact and blast loading were also performed using the computer code.

## 2. High strain-rate effects and constitutive models for concrete

In general, the mechanical response of any structural material is dependent on the strain rate. The rate sensitivity of concrete plays a considerable role in its dynamic load capacity. By increasing the strain rates, the strength of concrete is significantly increased in both tension and compression. Therefore, strain rate effects should be taken into account for realistically simulating concrete behaviour under high loading rates.

In order to perform a progressive failure analysis of a concrete structure, i.e., to trace the overall response up to the ultimate state, complete constitutive relations must be known not only including the pre-peak behaviour but also the post-failure response. The reasons are that the local failure of some components of a concrete structure subjected to blast and impact loading does not imply the collapse of the whole structure. Also the blast resistant design based on neglecting the strength degradation can be very uneconomical. Therefore, it is very important to include the rate dependent material nonlinearities (pre-peak and post-peak behaviour) of concrete and steel in the material model. The progressive concrete cracking and the concrete material nonlinearities in the pre-failure and post-failure regimes in compression as well as in tension should be simulated using suitable rate dependent rules.

For concrete structures subjected to blast or impact effects, a response at very high strain-rates is often sought. At these high strain-rates, the strength of concrete can increase significantly. The CEB-FIP (1990) model for strain rate effect is a widely accepted model for predicting the dynamic increase factor (DIF) for the peak compressive stress ( $f'_c$ ), (Eqs. (1) and (2))

$$\left(\frac{f_c}{f_{cs}}\right) = DIF = \left(\frac{\dot{\varepsilon}}{\dot{\varepsilon}_s}\right)^{1.026\alpha} \quad \text{for } \dot{\varepsilon} \leq 30s^{-1} \quad (1)$$

$$\left(\frac{f_c}{f_{cs}}\right) = DIF = \gamma \left(\frac{\dot{\varepsilon}}{\dot{\varepsilon}_s}\right)^{1/3} \quad \text{for } \dot{\varepsilon} > 30 \text{ s}^{-1} \quad (2)$$

where,  $\dot{\varepsilon}$  : strain rate  
 $\dot{\varepsilon}_s$  :  $30 \times 10^{-6} \text{ s}^{-1}$  (quasi-static strain rate)  
 $\log \gamma$  :  $6.156 \alpha - 2$   
 $\alpha$  :  $1/(5 + 9 f'_c/f'_{co})$   
 $f'_{co}$  : 10 MPa = 1450 psi

A series of impact tests were carried out by Ngo (2005), based on the Split Hopkinson Pressure Bar (SHPB) set-up, using large-diameter concrete cylinders to achieve a range of loading rates and hydrostatic pressures. Concrete specimens with different strengths (from 32 MPa to 160 MPa) were tested. It was found that the transition strain-rate is dependent on the concrete strength and should not be fixed at  $30 \text{ s}^{-1}$  as suggested by the CEB-FIP model in Eqs. (1) and (2). The CEB-FIP model was also found not applicable to high and ultra high strength concretes (with compressive strength above 100 MPa).

Based on the results of the experimental program using Hopkinson Bar apparatus, and through a rigorous calibration process, a new strain-rate dependent constitutive model is proposed by the authors. This new model is based on the format of the CEB-FIP model using parameters which were calibrated with the results from the SHPB carried out by the authors (Ngo 2005) and other data (Bichoff and Perry 1991). This proposed model applies to concrete under a dynamic load, and takes into account the strain-rate effect by incorporating multiplying factors for increases in the peak stress and strain at peak strength. This model is applicable to concrete strengths varying from 32 MPa to 160 MPa with a strain-rate up to  $300 \text{ s}^{-1}$ . In this model, the rate dependent peak compressive stress ( $f'_{cd}$ ) can be expressed as

$$K_{cd} = \frac{f'_{cd}}{f'_{cs}} = \left(\frac{\dot{\varepsilon}}{\dot{\varepsilon}_s}\right)^{1.026\alpha} \quad \text{for } \dot{\varepsilon} \leq \dot{\varepsilon}_1 \quad (3)$$

$$K_{cd} = \frac{f'_{cd}}{f'_{cs}} = A_1 \ln(\dot{\varepsilon}) - A_2 \quad \text{for } \dot{\varepsilon} \leq \dot{\varepsilon}_1 \quad (4)$$

where,  $f'_{cs}$  : static compressive strength (MPa)  
 $\dot{\varepsilon}$  : strain-rate  
 $\dot{\varepsilon}_s$  :  $3 \times 10^{-5} \text{ s}^{-1}$  (quasi-static strain-rate)  
 $\alpha$  :  $1/(20 + f'_{cs}/2)$   
 $\dot{\varepsilon}_1$  :  $0.0022 f'^2_{cs} - 0.1989 f'_{cs} + 46.137$   
 $A_1$  :  $-0.0044 f'_{cs} + 0.9866$   
 $A_2$  :  $-0.0128 f'_{cs} + 2.1396$

Fig. 1 shows the DIF curves plotted using the proposed model for three concrete groups: NSC, HSC and RPC. Test results are also plotted to compare with the proposed model. It should be noted that in the above formulae, the turning point strain-rate,  $\dot{\varepsilon}_1$ , is a function of the static compressive strength  $f'_{cs}$ .

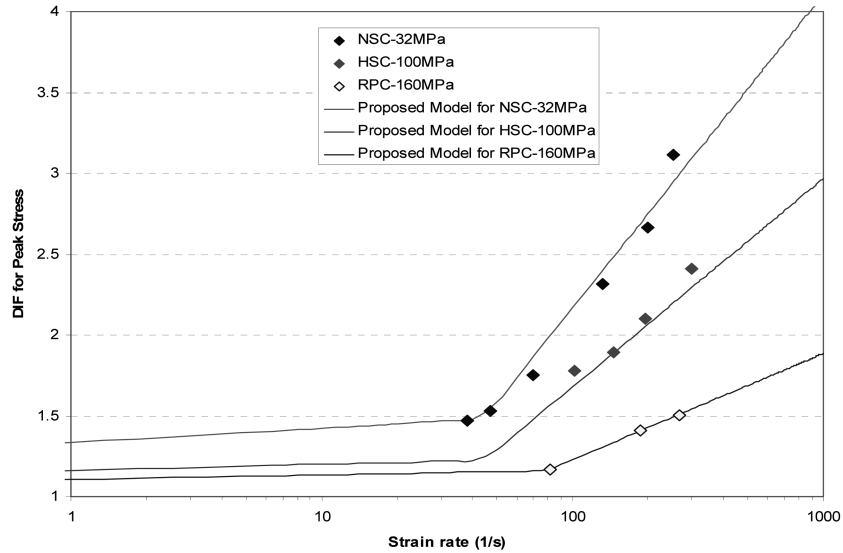


Fig. 1 Proposed DIF model for peak stress

### 3. Modelling capabilities of the Rate Dependent Lattice Concrete Model (RDLM)

The discrete lattice model was initially developed by Niwa *et al.* (1994). This model has been successfully used to model RC structures under cyclic loading (Itoh *et al.* 2000). The discrete lattice model was extended by Tanabe and others (Tanabe and Ishtiaq 1999, Itoh *et al.* 2000), so as to be able to model continuum RC structures using a finite element method. In the equivalent continua lattice model (ECLM) a RC structure can be modelled as parallel layers of concrete and

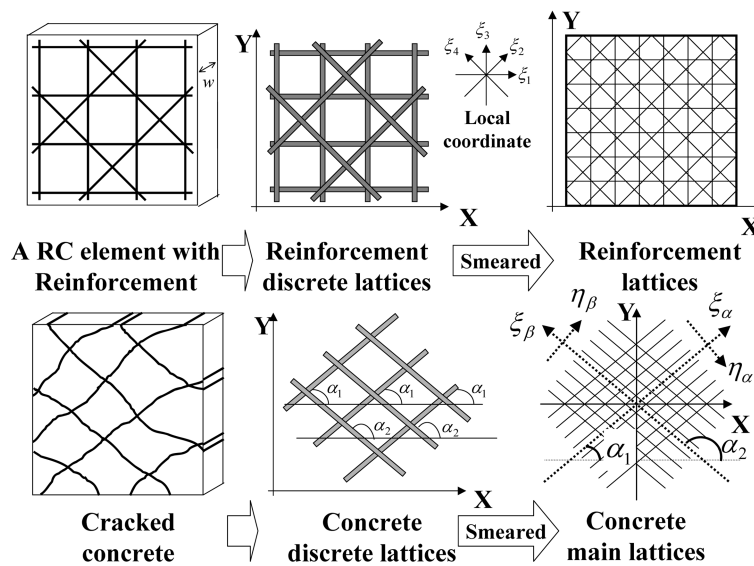


Fig. 2 Lattice model

reinforcement lattices, as shown in Fig. 2 (Tanabe and Ishtiaq 1999). This model can be expressed using the finite element (FE) formulation, by smearing out concrete and reinforcement lattices into a continuum. The equivalent continua lattice model has been used successfully in modelling RC columns subject to quasi-static and cyclic loadings (Itoh and Tanabe 2002).

The ECLM has shown the following capabilities of modelling reinforced concrete behaviour:

- Concrete strain softening regime to simulate the post-failure behaviour in compression until crushing.
- Concrete tensile cracks which represent the main source of material nonlinearity.
- Tension softening and tension stiffening in the post-cracking behaviour.
- Crack interface shear transfer.

However the ELCM does not take into account the strain rate effects thus limiting its capability to model concrete structures subjected to blast or high velocity impact. In this study, the ECLM was improved to include the strain rate effects. The proposed model called Rate Dependent Lattice Model (RDLM) incorporates a strain rate sensitive lattice model for both compressive and tensile behaviour of concrete and steel reinforcement. The FE formulation of the proposed model is described in detail by Ngo (2005).

#### 4. The RDLM smear crack approach for finite element formulation

The smeared crack model was adopted for the finite element (FE) formulation of the rate dependent lattice model (RDLM). In this approach cracked concrete is assumed to remain a continuum and the material properties are modified to account for the damage due to cracking. The smeared crack model has been chosen for the following reasons:

1. For impulsive loading conditions where the cracking patterns are difficult to predict, and also for situations where the scale of the representative continuum is large compared to the crack spacing, the smeared concept provides a realistic approach for distributed fracture representation compared with the discrete model which seems adequate only for simple problems involving a few dominant cracks.
2. The proposed constitutive lattice models presented in the previous section can easily be implemented in the smeared crack approach. They are also suitable for the description of concrete behaviour at the macroscopic level but not at the microscopic level where the discrete crack approach may be more appropriate.
3. The simplicity and the computational advantages of the smeared crack approach allow crack initiation in any direction as well as the automatic generation of cracks without predefining or redefining the finite element mesh.

The constitutive equation for the RDLM is comprised of six lattice components. These include compressive and tensile concrete lattices, longitudinal and transverse reinforcement lattices, and two shear lattices, to evaluate the shear transfer on the crack surfaces. The main lattice  $[D_{main}]$  includes the concrete and reinforcement lattices, which are then combined with the shear lattices  $[D_{shear}]$  to obtain the total stiffness matrix  $[D_{total}]$  of the constitutive equation for the model; i.e.

$$[D_{total}] = [D_{main}] + [D_{shear}] \quad (5)$$

Eq. (5) is the general form of the constitutive equation for the RDLM. The stress-strain relationship for the lattices is described below.

#### 4.1 Main lattice

The stress-strain matrix of a cracked reinforced concrete element is expressed by assuming a uniformly strained 2D continuum. The local strains in each lattice component are calculated from which the stress vectors in the local coordinate are evaluated using the uniaxial stress-strain relationship of each lattice component. The equivalent stress-strain matrix in the global coordinate system, which is the general form of the constitutive equation for main lattice, is expressed as

$$\Delta\{\sigma_g\} = [L_\varepsilon]^T [R_n] [L_\varepsilon] \Delta\{\varepsilon_g\} = [D_{main}] \Delta\{\varepsilon_g\} \quad (6)$$

In Eq. (6), the stiffness matrix  $[D_{main}]$  for the main lattice in the RDLM is written as

$$[D_{main}] = \begin{bmatrix} \sum_1^n E_i t_i \cos^4 \alpha_i & \sum_1^n E_i t_i \cos^2 \alpha_i \sin^2 \alpha_i & \sum_1^n E_i t_i \cos^3 \alpha_i \sin \alpha_i \\ & \sum_1^n E_i t_i \sin^4 \alpha_i & \sum_1^n E_i t_i \cos \alpha_i \sin^3 \alpha_i \\ \text{symm.} & & \sum_1^n E_i t_i \cos^2 \alpha_i \sin^2 \alpha_i \end{bmatrix} \quad (7)$$

The values of  $t_i$  are the thickness ratios of each lattice component that are smeared out and the subscript  $i$  denotes the number of elements in the  $Z$  direction (element width direction).  $\alpha_i$  is the angle of inclination of each lattice to global coordinate.

#### 4.2 Shear lattice

The shear transfer mechanism along the crack surface is shown in Fig. 3. To model the effect aggregate interlock in the RDLM, two shear lattices  $S1$  and  $S2$  are provided. The effect of aggregate interlock is dependent on the relative movement of concrete on two sides of the crack. The aggregate interlock will occur in two ways. On one hand, the interlocking effect, due to the collision of a side of both surfaces as shown in Fig. 3 with acute angle, will be activated for plus shear direction, while the surface of the crack of obtuse angle will be activated for minus shear direction on the other hand. In each of these interlocking effects, two elements of shear lattices  $S1$  and  $S2$  are allocated in perpendicular direction to the surface, which will carry the shear forces along a crack. The dowel effect can be accounted for by changing the inclination angles of the reinforcement lattice components in proportion to the progress of fracture.

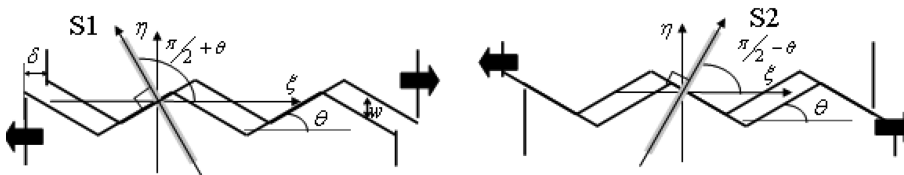


Fig. 3 Shear transfer model

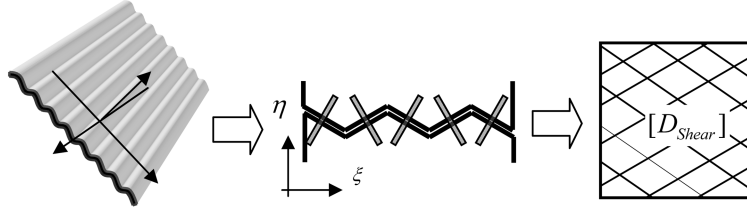


Fig. 4 FE formulation of shear lattices

The local coordinate defining the crack surface ( $\eta, \xi$ ) is shown in Fig. 4. The rigidity of the shear lattices in the local coordinate system is denoted as  $D_{shear, \xi \eta}$ . To transform this into global coordinate system, the shear controlling matrix  $\Omega$  and global coordinate transformation matrices  $T_1, T_2$  are used to define the global shear stiffness matrix  $D_{shear}$  as follows

$$[D_{shear}] = [T_1][\Omega][D_{shear, \xi \eta}][T_2] \quad (8)$$

## 5. Material model for lattice components

### 5.1 Model for concrete in compression

A rate dependent compressive concrete model with a pronounced post-peak decay has been developed in this study. Under the bi-axial state of stress, compressive cracked concrete includes the softening of compressive concrete due to the presence of transverse tensile strains. The softening coefficient  $\eta$  is considered to be unity at the uniaxial state of stress. The concrete stress-strain relationship in compression is shown in Fig. 5 and is expressed as follows

$$f_{cd} = \eta K_{cd} f'_{cs} \left[ \frac{2\varepsilon}{\varepsilon_{cd}} - \left( \frac{\varepsilon}{\varepsilon_{cd}} \right)^2 \right] \quad \text{for } \varepsilon \leq \varepsilon_{cd} \quad (9)$$

$$f_{cd} = \eta [K_{cd} f'_{cs} - Z_d(\varepsilon - \varepsilon_{cd})] \quad \text{for } \varepsilon > \varepsilon_{cd} \quad (10)$$

where,  $f_{cd}$  : compressive dynamic strength under high strain rate (MPa)

$K_{cd}$  : dynamic increase factor for compressive strength (MPa) (obtained from Eqs. (3) and (4))

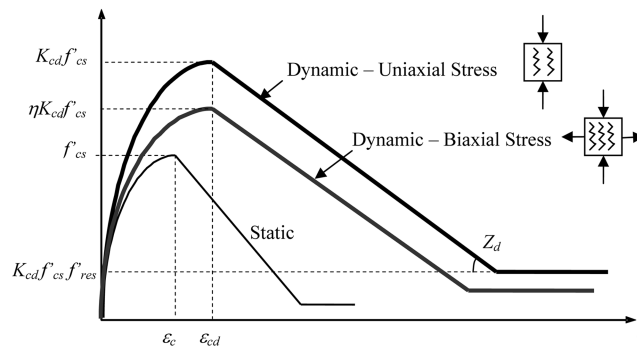


Fig. 5 Concrete stress-strain model under compression

$\varepsilon$  : principle compressive strain of concrete  
 $\varepsilon_{cd}$  : dynamic strain at peak stress =  $\varepsilon_{cs}(-0.00002 f'_{cs} + 0.0057) \dot{\varepsilon}$   
 $\varepsilon_{cs}$  : static strain at peak stress =  $\frac{4.26}{\sqrt[4]{f'_{cs}}} \frac{f'_{cs}}{E_{cs}}$   
 $\eta = \frac{1.0}{0.8 - 0.34(\varepsilon_1/\varepsilon_{cd})} \leq 1.0$

In the strain-softening region, it is assumed that the stress reduces linearly to  $K_d f'_c f'_{res}$ . In this study the residual strength  $f'_{res}$  is taken as 0.2. Unloading is modelled to decrease with the initial coefficient. On the other hand, in the reloading path, the stress is assumed to increase linearly to the post maximum stress point in the previous stress history.

5.2 Model for concrete in tension

Concrete is assumed to be an elastic material before cracking. In order to incorporate some ductility in the post-cracking region, a bi-linear tension softening model, as shown in Fig. 6, is adopted. A dynamic increase factor,  $K_{td}$ , for tensile concrete proposed by Malvar and Ross (1998) is adopted to account for strain rate effect. Thus the dynamic tensile strength of concrete is as follows

$$f_{td} = K_{td} f_{ts} \tag{11}$$

$$K_{td} = \left(\frac{\dot{\varepsilon}}{\dot{\varepsilon}_s}\right)^{1.016\delta} \quad \text{for } \dot{\varepsilon} \leq 1 s^{-1} \tag{12}$$

$$K_{td} = \beta \left(\frac{\dot{\varepsilon}}{\dot{\varepsilon}_s}\right)^{1/3} \quad \text{for } \dot{\varepsilon} > 1 s^{-1} \tag{13}$$

where,  $f_{ts}$  : static tensile strength of concrete (MPa)  
 $\dot{\varepsilon}$  and  $\dot{\varepsilon}_s$  : strain rate up to  $160 s^{-1}$  and quasi-static strain rate respectively  
 $\log \beta = 6 \delta - 2$ ;  $\delta = 1/(8 + 8 f'_{cs}/f_{co})$ ; and  $f_{co} = 10$  MPa

5.3 Bond effects and tension stiffening

The tension stiffening effect in the cracked reinforced concrete, as shown in Fig. 7, due to bond

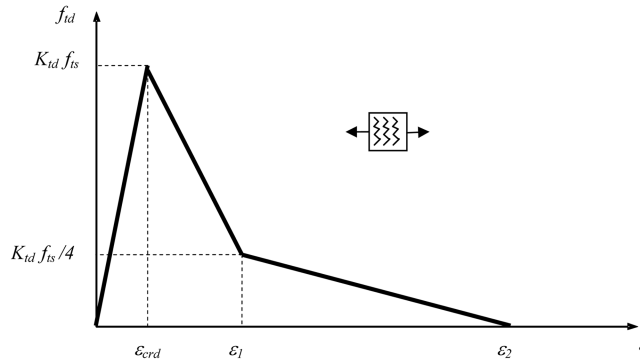


Fig. 6 Concrete stress-strain model under tension

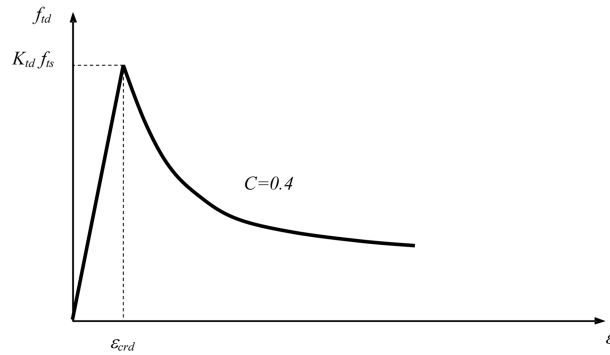


Fig. 7 Tension stiffening model

effect is also considered to be rate dependent and is given by

$$f_{id} = K_{id} f_{ts} \left( \frac{\epsilon_{crd}}{\epsilon} \right)^C \tag{14}$$

The bond effect coefficient,  $c$ , is assumed to be 0.4 in this study. The unloading and reloading paths of the tensile model are similar to the concrete model for compression.

#### 5.4 Model for steel reinforcement

The stress-strain relationship of reinforcement is expressed by a bilinear model, representing elasto-viscoplastic behavior with linear isotropic hardening and is assumed to be identical in tension and compression (Fig. 8). In the elastic range, the material behavior is rate independent and linear until the yield stress, which is strain rate dependent, is reached. The rate effects are considered to be equal in both tension and compression. The dynamic increase factor (DIF) for yield stress ( $f_{yd}$ ) recommended by Malvar (1998) is adopted in this study as follows

$$f_{yd} = f_{ys} \left( \frac{\dot{\epsilon}}{10^{-4}} \right)^\alpha \tag{15}$$

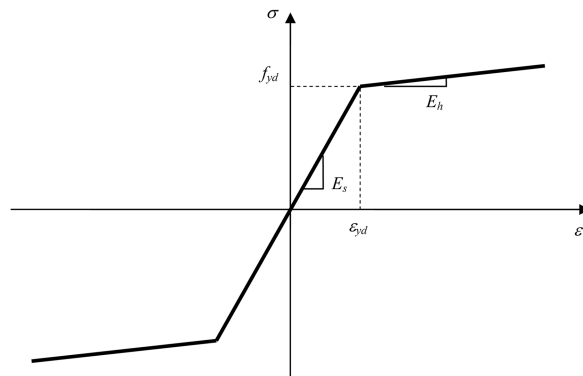


Fig. 8 Reinforcement model

$$\alpha = 0.074 - 0.04 \frac{f_{ys}}{414} \quad (16)$$

where,  $f_{ys}$  : static yield strength of steel (MPa)  
 $f_{yd}$  : dynamic yield strength of steel (MPa)  
 $\dot{\varepsilon}$  : strain rate of steel

## 6. Computer implementation and code validation

A computer program has been developed for the finite element linear and nonlinear transient dynamic analysis of two-dimensional reinforced concrete structures subjected to impulsive loading. The program is written in FORTRAN in modular form, and possesses sufficient flexibility to add new options resulting from further research. For time integration the program uses the central difference scheme. The explicit algorithm was optimized to reduce the computational time [more details are given by Ngo (2005)]. The program implements the rate-dependent continuum lattice model described above, combined with a tensile crack-monitoring algorithm. The algorithm, which traces the opening of new cracks as well as the closing and re-opening of existing ones, is activated after total and elastic evaluation for each sampling point at each time step. Compared to other material models available in commercial program such as LSDYNA (2007), the main advantage of the RDLM is that it requires small number of input parameters. These input parameters of the RDLM can also be derived from the conventional material tests.

In order to validate the material models and the explicit code, analytical results are compared with the experimental results from the impact tests conducted by Agardh *et al.* (1999) and with the Ultra High Strength Concrete (UHSC) panels tested during the Woomera blast trial in May 2004. The results from the blast trial are presented in detail in Ngo *et al.* (2007). The finite element modelling results and comparisons with the test data are presented in this section.

### 6.1 Reinforced concrete beams under impact loading by Agardh *et al.* (1999)

Five high strength concrete beams of 4200 mm × 340 mm × 170 mm dimensions were subjected to a drop weight of 718 kg striking the middle section of the beams with a velocity of 6.7 m/s. The main material properties of concrete and steel employed in the analysis are listed in Table 1. The

Table 1 Material properties of concrete and steel

	Material properties	Agardh <i>et al.</i>	UHSC panels
Concrete	Compressive strength, $f'_c$ (MPa)	112	164.2 MPa
	Tensile strength, $f_t$ (MPa)	6.7	22.8
	Elastic modulus, $E_c$ (GPa)	45.3	44.1
	Poisson's ratio, $\nu$	0.3	0.3
	Mode I fracture energy, $G_f$ (N/m)	156	325
Longitudinal reinforcement	Elastic modulus, $E_s$ (GPa)	207	198
	Yield stress, $f_y$ (MPa)	586	1680 (prestressed)
Transverse stirrup	Elastic modulus, $E_s$ (GPa)	207	
	Yield stress, $f_y$ (MPa)	586	

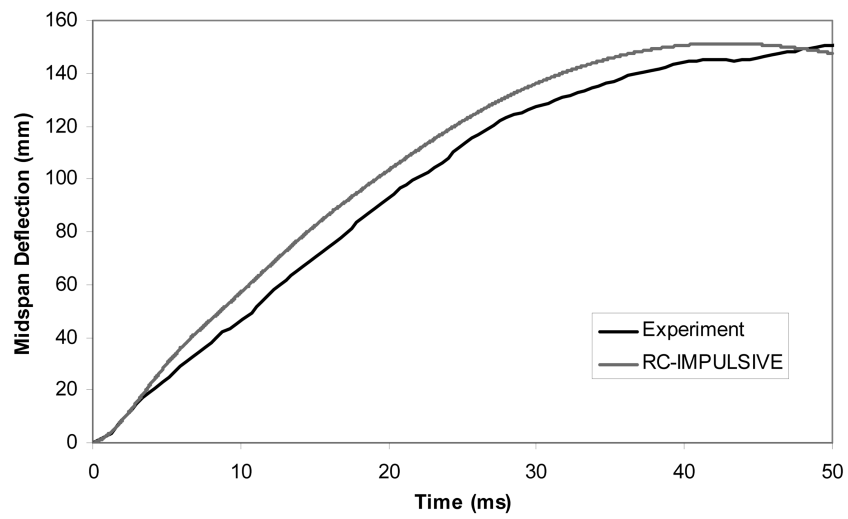


Fig. 9 Comparison of midspan deflections

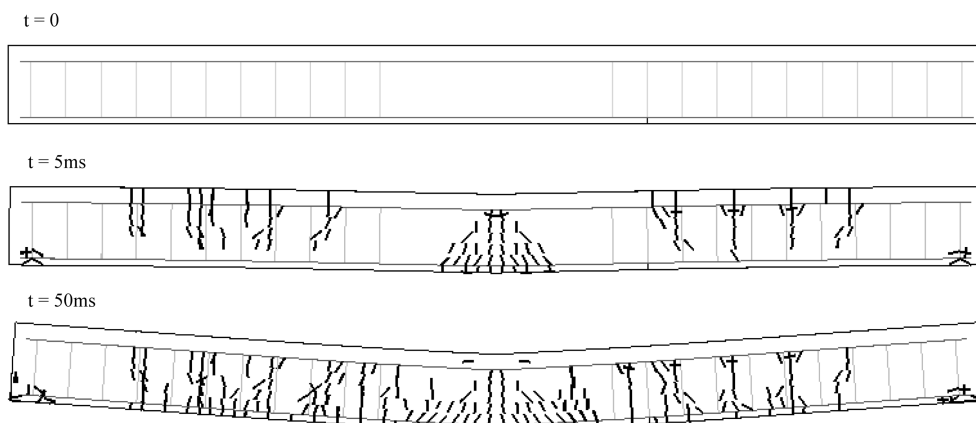


Fig. 10 Crack patterns of the HSC beam predicted by the RDLM

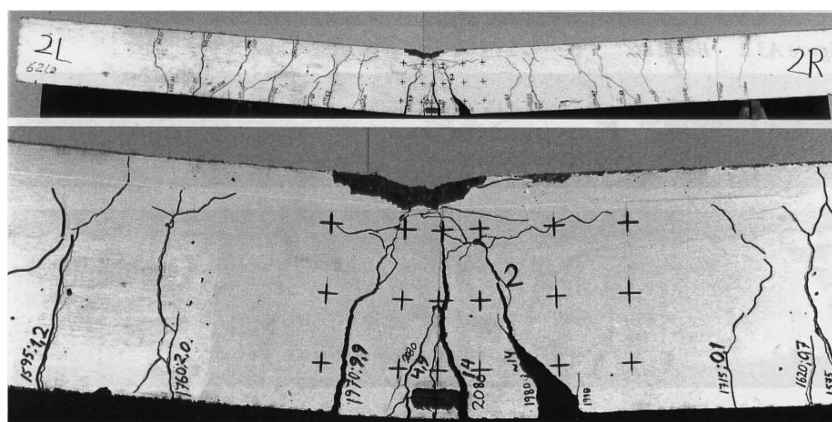


Fig. 11 Crack pattern of the HSC beam after impact

displacements were recorded with a 16 mm, high speed video camera with 1500 frames/sec. Reinforcement strains of bottom bars, accelerations at top of the beams and velocities of the drop weight were also recorded. The dynamic analysis is performed with a time step of 5 micro seconds and no viscous damping has been considered. The analytical model consists of 595 nodes, 504 four-node elements and 202 truss elements. Fig. 9 shows the time history of the mid-span deflection predicted by the explicit code and the experimental results and is found to be in good agreement with the experimental results. The crack pattern predicted by this program including both flexural and shear cracks also follows the crack pattern observed in the impact tests (Figs. 10 and 11).

### 6.2 UHSC panels subject to blast loading

A total of three Ultra High Strength Concrete (UHSC) panels were prepared for the blast trial at Woomera, South Australia, in May 2004. Each panel has the dimension of  $1000 \times 2000$  mm. The panel thicknesses are 75 mm and 100 mm. The one-way UHSC panels, supported only on two vertical sides, are modelled as simply supported beams with a span of 2 m. The panels were prestressed to 20% of the ultimate strength of the tendons. Concrete is modelled using plane stress elements with four nodes. The prestressed tendon is simulated as perfectly bonded truss elements. The FE model includes 205 nodes, 160 four-node elements and 40 truss elements. The prestressed effects are modelled by setting initial tensile stresses for steel elements, as well as initial compressive stresses for concrete elements. The time step length is chosen to be 2.5 micro-seconds. The result for the UHSC panel No. 1 is presented here. The main material properties of concrete and steel employed in the analysis for the panel are listed in Table 1.

UHSC Panel No. 1 is a 100 mm thick prestressed UHSC panel located at 30m stand-off distance. The blast results in an average reflected impulse at the panel surface equal to 3771 kPa.msec with an average reflected pressure of 1513 kPa. The computed displacement-time history and experimental measurements at the mid-span of the UHSC Panel No.1 are plotted for comparison in Fig. 12 which shows very good agreement. The peak inward deflection of 50.4 mm was recorded

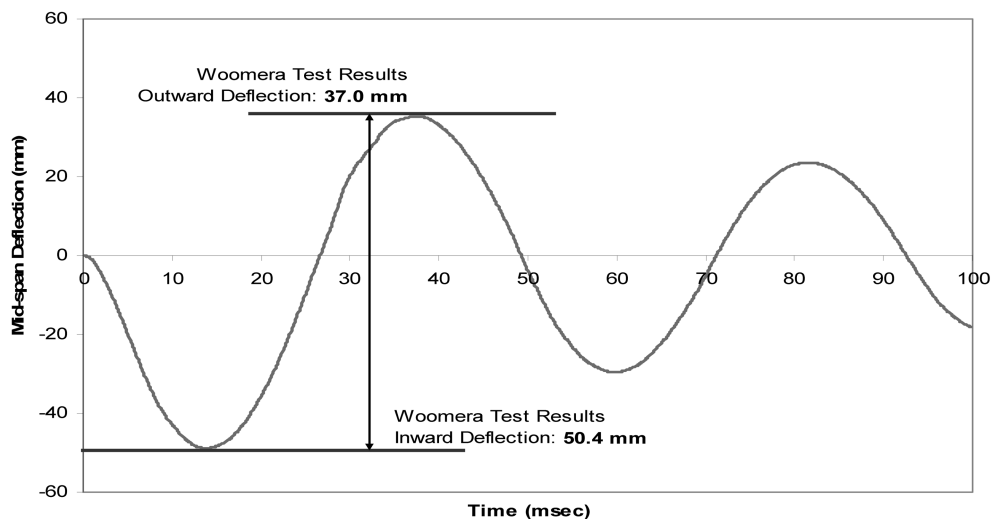


Fig. 12 Mid-span deflection history of 100 mm thick UHSC Panel No.1 at 30 m predicted by the RDLM compared with the Woomera test results

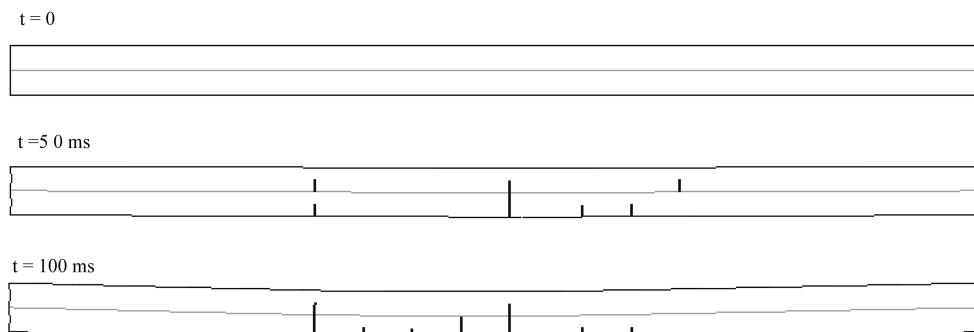


Fig. 13 Crack patterns of the UHSC Panel No.1 predicted by the RDLM



Fig. 14 Crack pattern of the UHSC Panel No.1

which agrees closely with the analytical results, for which the computed peak inward displacement of 48.6 mm is reached in 14.4 msec. Again there is good agreement between the computed peak outward displacement of 35.3 mm reached at time  $t = 37.9$  msec, compared with the recorded deflection of 37.0 mm.

The deformed shape of the UHSC Panel No.1 at different time intervals is plotted in Fig. 13 in which the crack patterns of concrete at various stages in the loading history of the panel are also displayed. These results match the experimentally recorded crack pattern in Fig. 14 quite well on both front and rear faces. It may be further observed that although there is some diffusion in the crack pattern, as in all smeared crack analysis, strain localisation is clearly monitored. Similar to the experimental behavior, only minor cracks are developed and concrete crushing does not occur for this panel.

## 7. Conclusions

The inclusion of strain rate effects on the proposed rate dependent lattice models for concrete and steel leads to a realistic nonlinear dynamic analysis of reinforced concrete structures under impulsive loading conditions. The computer program developed in this study is shown to be capable

of modelling the nonlinear dynamic behaviour of reinforced concrete structures where deformations, stresses, and the progressive fracture in concrete and steel can be traced. The dynamic response of the test panels under blast loading, as predicted by the explicit code, shows that an accurate numerical simulation of the experimental observations is possible using the proposed nonlinear numerical method, despite the highly variable nature of the loading conditions.

## References

- Agardh, L., Magnusson, J. and Hansson, H. (1999), "High strength concrete beams subjected to impact loading", Research Report, Defense Research Establishment FOA, Sweden.
- Bichoff, P.H. and Perry, S.H. (1991), "Compressive behaviour of concrete at high strain rates", *Mater. Struct.*, **24**, 425-450.
- CEB-FIP (1990), *CEB-FIP Model Code 1990*, Comité Euro-International du Béton, Redwood Books, Trowbridge, Wiltshire, UK.
- Itoh, A. and Tanabe, T. (2002), "Analysis of RC column experiments at UCSD by an equivalent lattice model", Research Report, Dept. of Civil Engineering, Nagoya University, Japan.
- Itoh, A., Niwa, J. and Tanabe, T. (2000), "Evaluation by lattice model of ultimate deformation of RC columns subjected to cyclic loading", *Proceedings of JSCE*, No.641/V-46.
- LS-DYNA Version 971. (2007), Livermore Software Technology Corporation.
- Malvar, L.J. and Ross, C.A. (1998), "Review of strain-rate effects for concrete in tension", *ACI Mater. J.*, **95**(6), 735-739.
- Malvar, L.J. (1998), "Review of static and dynamic properties of steel reinforcing bars", *ACI Mater. J.*, **95**(5), 609-616.
- Ngo, T. (2005), "Behaviour of high strength concrete subjected to impulsive loading", PhD Thesis, Department of Civil & Environmental Engineering, University of Melbourne, Australia.
- Ngo, T., Mendis, P. and Krauthammer, T. (2007), "Behavior of ultrahigh-strength prestressed concrete panels subjected to blast loading", *J. Struct. Eng. ASCE*, **133**(11), 1582-1590.
- Niwa, J., Choi, I.C. and Tanabe, T. (1994), "Analytical study for shear resisting mechanism using lattice model", *JCI International Workshop on Shear in Concrete Structures*, 130-145.
- Tanabe, T. and Ishtiaq, A.S. (1999), "Development of lattice equivalent continuum model for analysis of cyclic behaviour of reinforced concrete", Seminar on Post-peak Behaviour of RC Structures Subjected to Seismic Load, **2**, 105-123.